

Critical quantum metrology in a stabilized two-photon Rabi model

Zu-Jian Ying,^{1,2,*} Hang-Hang Han,^{1,2} Bo-Jian Li,^{1,2} Simone Felicetti,^{3,4,†} and Daniel Braak^{5,‡}

¹*School of Physical Science and Technology, Lanzhou University, Lanzhou 730000, China*

²*Key Laboratory for Quantum Theory and Applications of MoE,*

Lanzhou Center for Theoretical Physics, Lanzhou University, Lanzhou 730000, China

³*Institute for Complex Systems, National Research Council (ISC-CNR), 00185 Rome, Italy*

⁴*Physics Department, Sapienza University, 00185 Rome, Italy*

⁵*TP III and Center for Electronic Correlations and Magnetism,
University of Augsburg, 86135 Augsburg, Germany*

We investigate a generalized quantum Rabi model (QRM) with two- and four-photon terms with respect to applications for non-linear critical quantum metrology. In the introduced model, the spectral collapse occurring in the standard two-photon QRM is stabilized by the presence of the quartic potential. The collapse is then transformed into a quantum phase transition, which occurs in the low-frequency limit of the light mode, whose remnant at finite ratio between qubit and mode frequencies can be applied to critically enhanced quantum metrology. We find that the four-photon term entails a much higher measurement precision compared to the standard two-photon QRM. The mechanism behind the higher precision can be traced to the different behavior of the ground state wave function as the system is tuned through the transition. As the standard two-photon QRM, despite the absence of the spectral collapse, our model allows for a finite preparation time for the probe state (PTPS).

PACS numbers:

I. INTRODUCTION

Quantum metrology and sensing are based on the use of quantum resources [1, 2] to overcome the performance of any classical strategy. Critical quantum sensing (CQS) is by now a well established approach, which makes use of the quantum properties spontaneously developed by critical systems in proximity of quantum phase transitions. Indeed, it has been theoretically shown that a quantum-enhanced sensing precision can be achieved exploiting static [3–13] or dynamical [14–17] properties of many-body systems in proximity of the critical point. In spite of the critical slowing down, the optimal precision scaling can be achieved not only with respect to the system probe size, but also with respect to protocol duration time [18]. Furthermore, when using adaptive strategies [19–21], CQS protocols are efficient also for global quantum sensing. The practical relevance of the CQS approach is confirmed by the first experimental implementations, carried out with Rydberg atoms [22], nuclear magnetic resonance [23] and superconducting quantum circuits [24–26].

Of particular interest for this work, CQS protocols can also be conceived [27] considering finite-component phase transitions (FCPTs) [28–49], which are quantum criticalities formally obtained by applying a scaling limit on the system parameters [33, 37, 39, 50, 51]. FCPTs have been mainly studied considering quantum resonators with embedded atomic [28, 30, 52–55] or Kerr [51, 56–59] non-

linearities, and they have been controllably implemented using atomic systems [60], polaritonic systems [61, 62] and superconducting quantum systems [63–68]. FCPTs provide a tractable framework to analyze the performance of CQS protocols. For example, they have been used to demonstrate the constant-factor advantage of dynamical over statical protocols [69, 70], to unveil the presence of apparent super-Heisenberg scalings [71–73], to analyze continuous-measurement schemes [74, 75], and to make formal comparison with passive quantum sensing strategies [76]. This framework has been used to design CQS protocols which can be implemented with small-scale devices, considering systems based on parametric resonators [24, 77–82], trapped-ions [83], optomechanical [84, 85] or magnomechanical [86] devices, spin defects [87, 88] and Rabi systems [89–94].

An interesting class of finite-component models is given by two-photon or quadratic couplings, where quantum emitters interact with bosonic modes exclusively via the exchange of excitation pairs. These models can be feasibly implemented with atomic [95] and solid-state [96–101] quantum technologies. Two-photon interactions lead to an interesting phenomenology [34, 35, 102–105] and they can induce quantum phase transitions in both extended [27, 106–108] and finite-component models [34, 35, 109]. It has already been shown that two-photon couplings can be effectively deployed in critical quantum sensing protocols [89, 93, 94]. Two-photon couplings are known to induce a spectral collapse, where the discrete spectrum collapses into a continuous energy band [110–114]. Although the onset of the collapse can in principle be observed [95, 97], beyond the collapse point the model is unbounded from below and so becomes un-

* yingzj@lzu.edu.cn

† simone.felicetti@cnr.it

‡ daniel.braak@uni-a.de

stable.

Here, we introduce a generalized two-photon quantum Rabi model (QRM) that is stable in the whole parameter space. In particular, we include a quartic potential that transforms the spectral collapse in a quantum phase transition. We derive analytical solutions for the system eigenspectrum in the low-frequency limit and characterize the system critical behavior. Finally, we assess the metrological power of this model by evaluating the quantum Fisher information over the ground state manifold. We find that the quartic potential not only stabilizes the model, but it also enhances the achievable precision in a critical quantum sensing protocol.

The paper is organized as follows. In section II, the non-linear QRM with a quartic regulator term (A_4 term) is introduced. Section III shows that the quartic term removes the “spectral collapse”: The spectrum stays discrete for all parameter values. Section IV studies the quantum phase transition induced by the A_4 term in the slow-mode limit and gives analytic expressions for the transition point. Section V demonstrates a much enhanced QFI by the A_4 term, indicating higher measurement precision in quantum metrology as compared to the standard two-photon QRM. Section VI clarifies the mechanism of higher sensitivity effected by the A_4 term. Section VII shows that the PTPS stays finite for experimentally realizable parameter values and section VIII presents concluding remarks.

II. MODEL

The (extended) two-photon QRM is described by the following Hamiltonian [34, 35]

$$H_T = \omega a^\dagger a + \frac{\Omega}{2} \hat{\sigma}_x + g_2 \hat{\sigma}_z [(a^\dagger)^2 + a^2 + \chi(2a^\dagger a + 1)] \quad (1)$$

which contains a quadratic coupling between the bosonic mode with frequency ω , created (annihilated) by a^\dagger (a), and a qubit represented by the Pauli matrices $\hat{\sigma}_{x,y,z}$. The simple two-photon QRM has $\chi = 0$, corresponding to two-photon absorption and emission processes. Including the Stark-like term [115] leads for $\chi = 1$ to the form $\hat{\sigma}_z (a^\dagger + a)^2$ which is realizable in superconducting circuit systems [96]. The \mathbb{Z}_4 -symmetry $P_4 = \hat{\sigma}_x e^{i\pi a^\dagger a/2}$ for $\chi = 0$ is broken down to \mathbb{Z}_2 for $\chi \neq 0$ [93], with symmetry operator $P_2 = e^{i\pi a^\dagger a}$ [37, 41, 93]. The Stark-like term leads to a rescaling of the critical coupling for spectral collapse [34, 35]

$$g_T = \frac{\omega}{2(1+\chi)}. \quad (2)$$

In the following, we set $\chi = 1$.

We augment now the Hamiltonian (1) by a term quartic in the boson operators, corresponding to four-photon processes,

$$H = \omega a^\dagger a + \frac{\Omega}{2} \hat{\sigma}_x + g_2 \hat{\sigma}_z (a^\dagger + a)^2 + A_4 (a^\dagger + a)^4, \quad (3)$$

which can be realized in superconducting circuit systems [116]. This term does not couple to the qubit degree of freedom, it can therefore be called “neutral” with respect to the qubit. Nevertheless it has a profound effect on the spectrum and the dynamical behavior of model. Here we have adopted the spin notation as in Ref. [117], in which the spin value in the z direction, $\sigma_z = \pm$, represents the two flux states in the flux-qubit circuit system [118]. This platform allows to realize the ultra-strong [119–136] and even deep-strong coupling regime [49, 131, 137, 138], with coupling strengths g_2 beyond 0.1ω and 1.0ω . In cavity QED systems Ω denotes the level splitting of the qubit and the model is usually written in a basis where the qubit is diagonal, corresponding to exchange of σ_x and σ_z .

III. ABSENCE OF SPECTRAL COLLAPSE

The model (1) with two-photon coupling exhibits the so-called “spectral collapse” phenomenon [95, 96, 112, 114, 139–141]. This is illustrated in Fig. 1(a), the energy levels of excited states E_i seem to collapse to a single energy E_{th} when the coupling g_2 reaches the critical value g_T . This apparent infinite degeneracy of E_{th} is a numerical artifact, caused by the necessarily finite dimension of the state space used in exact diagonalization of the model. In reality, the spectrum exhibits a *continuous* part, covering the whole real axis from E_{th} upward [114, 140]. Besides the continuum, the model (1) possesses at $g_2 = g_T$ infinitely many bound states below E_{th} , which are exponentially close to E_{th} and thus difficult to resolve by exact diagonalization [142].

The origin of the spectral collapse can be understood from a simple argument for the case $\Omega = 0$. Going to the \hat{x}/\hat{p} -representation via $a^\dagger = (\hat{x} - i\hat{p})/\sqrt{2}$, $a = (\hat{x} + i\hat{p})/\sqrt{2}$, where \hat{x} is the multiplication operator and $\hat{p} = -i\frac{\partial}{\partial x}$, we obtain [29, 34, 35, 117]

$$H_T = \sum_{\sigma_z = \pm} h_{\sigma_z} |\sigma_z\rangle \langle \sigma_z| + \frac{\Omega}{2} \sum_{\sigma_z = \pm} |\sigma_z\rangle \langle \bar{\sigma}_z| \quad (4)$$

where $\sigma_z = -\bar{\sigma}_z = \pm$ labels the spin state in z direction. Here $h_{\pm} = \frac{\omega}{2m_{\pm}} \hat{p}^2 + v_{\pm}(x) - \frac{1}{2}\omega$ is effective single-particle Hamiltonian, with effective mass $m_{\pm} = [1 \mp \frac{(1-\chi)g_2}{(1+\chi)g_T}]^{-1}$, in the spin-dependent potential [34, 35, 93, 112]

$$v_{\pm}(x) = \frac{1}{2}\omega \left(1 \pm \frac{g_2}{g_T}\right) x^2. \quad (5)$$

The spin-flip term proportional to Ω in (4) is relatively bounded with respect to the spin-diagonal term and plays no role in locating the critical point g_T . For $g_2 < g_T$, the quadratic potential is positive for both spin values, as illustrated in Fig. 2(a), leading to a purely discrete spectrum. However, in the $g_2 > g_T$ regime, the spin-down potential $v_-(x)$ is negative, as illustrated in

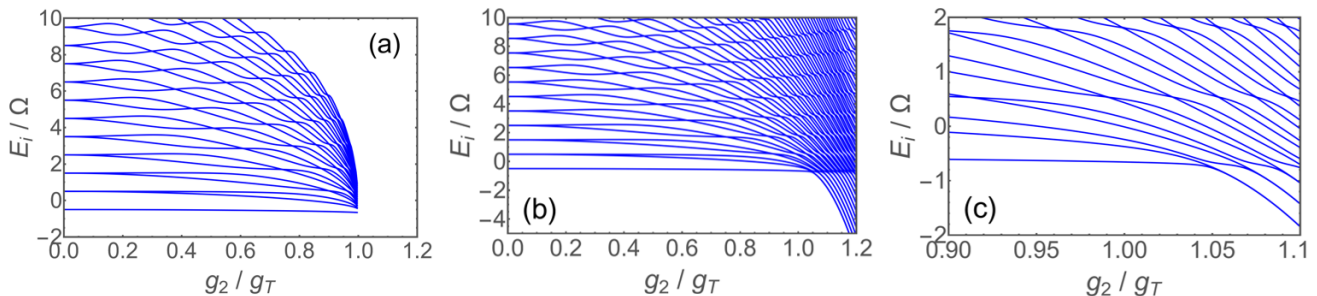


FIG. 1. The spectral collapse phenomenon. Energy spectrum E_i at $\omega = 1.0\Omega$: (a) $A_4 = 0$. The numerically computed levels seem to collapse to the single energy E_{th} at $g_2 = g_T$, with a single bound state remaining below E_{th} . In reality, the spectrum is continuous above E_{th} and the number of bound states is infinite. (b) $A_4 = 0.0001\omega$. The spectral collapse does no longer occur, because the effective potential is confining even though A_4 is very small. (c) A zoom-in plot around $\omega = 1.0\Omega$ of (b).

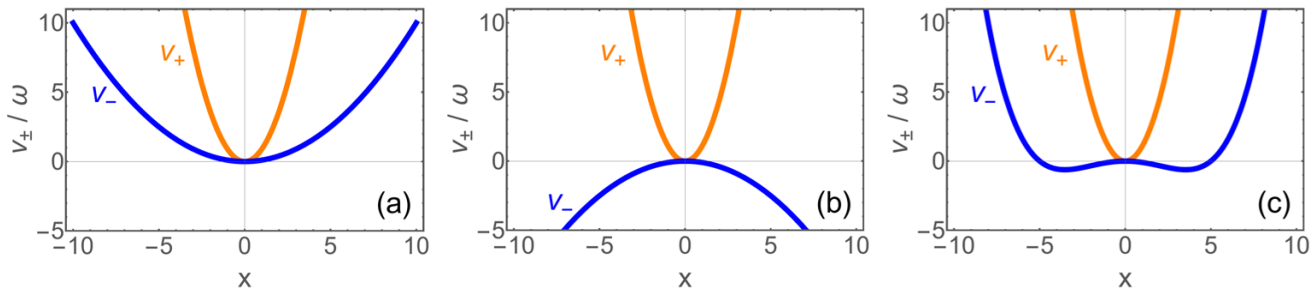


FIG. 2. Effective potential v_{\pm} for $\Omega = 0$: (a) $A_4 = 0$, $g_2 = 0.8g_T$. (b) $A_4 = 0$, $g_2 = 1.2g_T$. (c) $A_4 = 0.001$, $g_2 = 1.2g_T$.

Fig. 2(b), corresponding to an inverted harmonic oscillator (the parabolic barrier). The Hamiltonian is unbounded from below but still self-adjoint and generates a physically meaningful time evolution [143]. The spectrum is purely continuous, spanning the whole real axis from $-\infty$ to $+\infty$, similar to the spectrum of \hat{x} and \hat{p} . At the boundary $g_2 = g_T$, the spin-down potential $v_-(x)$ becomes flat, thus the spin-down sector exhibits a continuous spectrum for $\Omega = 0$. Whether this continuum persists and/or is modified for non-zero Ω , when both spin sectors are coupled, can be analyzed via the G -function technique [114, 142].

We have seen that the “collapse” is caused by an instability of the effective potential in the spin-down sector at $g_2 = g_T$. It can therefore be avoided by adding a positive potential which grows stronger than quadratically at infinity, namely the term $A_4(a^\dagger + a)^4 \sim \hat{x}^4$ in (3), as demonstrated in Fig. 1(b) where we have a purely discrete spectrum for any value of g_2 . The effective potential for $\Omega = 0$ reads now

$$v_{\pm}(x) = \frac{1}{2}\omega \left(1 \pm \frac{g_2}{g_T}\right) x^2 + 4A_4 x^4, \quad (6)$$

with $A_4 > 0$, as plotted in Fig. 2(c).

IV. QUANTUM PHASE TRANSITION IN THE SLOW-MODE LIMIT

A fascinating aspect of cavity QED is the presence of quantum phase transitions due to the infinite-dimensional Hilbert space of a single light mode [28–46, 48, 93]. Here we find that even in the absence of spectral collapse our non-linear system exhibits such a quantum phase transition, which can be inferred from the effective potential discussed in section III.

Indeed, in the $g_2 < g_T$ regime the (classical) particle tends to reside around the origin $x = 0$ which is the bottom of the potential as in Fig. 2(a), while beyond g_T the two potential minima have $x \neq 0$ corresponding to broken parity symmetry as in Fig. 2(c). Such a transition occurs in the slow-mode limit $\omega \ll \Omega$. In this situation the wave packet becomes so narrow relative to the potential size that it can be regarded as a semiclassical particle with large mass in an external field (the potential) while the quantumness of the two-level system is kept through the 2×2 matrix structure [35]. In such a picture the kinetic energy is neglected and the effective Hamiltonian reads

$$H_x = \begin{pmatrix} e_+(x) & \frac{1}{2}\Omega \\ \frac{1}{2}\Omega & e_-(x) \end{pmatrix}, \quad (7)$$

where $e_{\pm}(x) = \frac{1}{2}\omega \left(1 \pm \frac{g_2}{g_T}\right) x^2 + 4A_4 x^4$, which has a

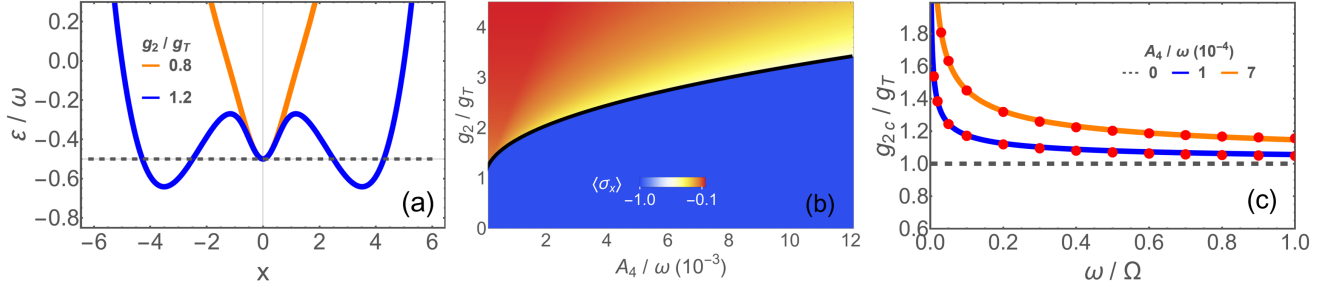


FIG. 3. Quantum phase transition. (a) Variational energy ε vs x in the semiclassical limit $\omega/\Omega \rightarrow 0$ at $g_2 = 0.8g_T$ [orange (light gray)] and $g_2 = 1.2g_T$ [blue (dark gray)]. (b) Phase diagram of $\langle\sigma_x\rangle$ (density plot) and analytic transition boundary g_{2c} by Eq.(10) (black solid line) vs A_4 at $\omega = 0.05\Omega$. (c) g_{2c} vs ω at $A_4 = 0.007\omega$ [orange (light gray)] and $A_4 = 0.001\omega$ [blue (dark gray)].

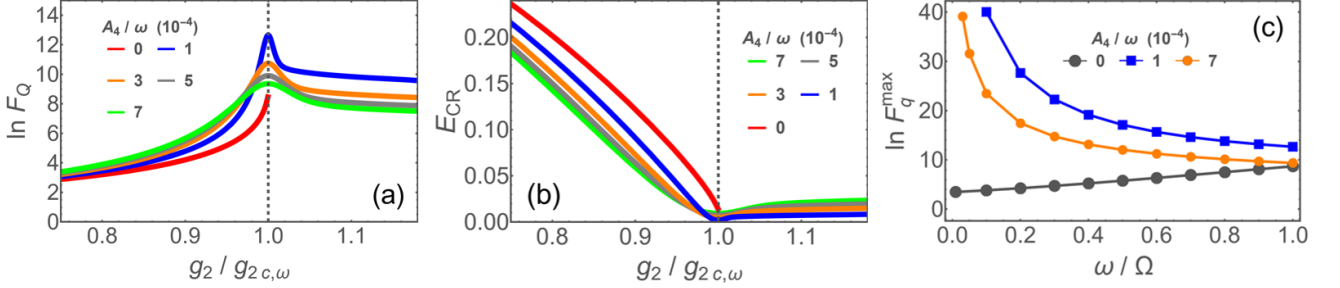


FIG. 4. Quantum Fisher information F_Q for quantum metrology. (a) F_Q in natural logarithmic scale for different values of A_4 at $\omega = 1.0\Omega$. (b) The Cramér-Rao error lower bound E_{CR} corresponding to (a). (c) Frequency dependence of the maximum values of F_Q at different values of A_4 . Here, $\lambda = g_2$ is taken as the measurement parameter for F_Q , g_2 is rescaled by the peak position $g_{2c,\omega}$ at frequency ω , and the unit scale of ratio A_4/ω is 10^{-4} .

lower energy branch

$$\varepsilon(x) = \frac{1}{2} \left[\omega x^2 + 8A_4 x^4 - \sqrt{\Omega^2 + \left(\frac{g_2}{g_T}\right)^2 \omega^2 x^4} \right]. \quad (8)$$

The energy minimum position x_{\min} is determined by the minimization of $\varepsilon(x)$. In Fig. 3(a) we plot two cases of $\varepsilon(x)$, where $\varepsilon(x)$ has a minimum at the origin for a weaker coupling $g_2 = 0.8g_T$ [orange (light gray)] while x_{\min} is away from the origin for a stronger coupling $g_2 = 1.2g_T$ [blue (dark gray)]. Thus, we see that upon increasing the coupling strength the transition occurs when the energy at x_{\min} is equal to the energy at the origin

$$\varepsilon(x_{\min}) = \varepsilon(0). \quad (9)$$

Equation (9) leads to the critical coupling ratio \bar{g}_{2c} ,

$$\bar{g}_{2c} \equiv \frac{g_{2c}}{g_T} = \sqrt{\frac{2}{3} + \frac{1 + 432\alpha_4}{3f^{1/3}} + \frac{1}{3}f^{1/3} + 16\alpha_4}, \quad (10)$$

where

$$f = 1080\alpha_4 - 1 + 24 \left(972\alpha_4^2 + \sqrt{6\alpha_4(54\alpha_4 - 1)^3} \right) \quad (11)$$

and $\alpha_4 = A_4\Omega/\omega^2$.

The validity of the analytic expression for g_{2c} in (10) is demonstrated in Fig. 3(b) where the black solid line, representing the analytic g_{2c} , matches the transition boundary of the spin expectation $\langle\hat{\sigma}_x\rangle$ extracted numerically from the minimization of $\varepsilon(x)$. Surprisingly, the validity of g_{2c} extends to finite ω , as shown in Fig. 3(c) where the analytic g_{2c} from (10) (solid lines) agrees with the transition points defined by the peak of the QFI (dots) [43] which will be subject of section V.

We may expand g_{2c} for small α_4 and large α_4 , respectively,

$$\bar{g}_{2c} \approx \sqrt{1 + 8\sqrt{2\alpha_4} + 24\alpha_4}, \quad (12)$$

$$\bar{g}_{2c} \approx \sqrt{\frac{2}{3} + 16\alpha_4 + 12\alpha_4^{2/3} + 4\alpha_4^{1/3} + \frac{\alpha_4^{-1/3}}{27} - \frac{\alpha_4^{-2/3}}{324}} \quad (13)$$

the former for small α_4 and the latter for large α_4 . We see that in both regimes the expansions manifest a fractional power law in α_4 . Such a fractional power law in the dependence of the critical coupling on the frequency ratio is also found in the linear quantum Rabi model [44]. There the fractional power law comes from the frequency renormalization of polarons, while here it stems from both nonlinear coupling terms, the quadratic and the quartic one. A comparison of the approximated forms with the full expression for g_{2c} is presented in Appendix

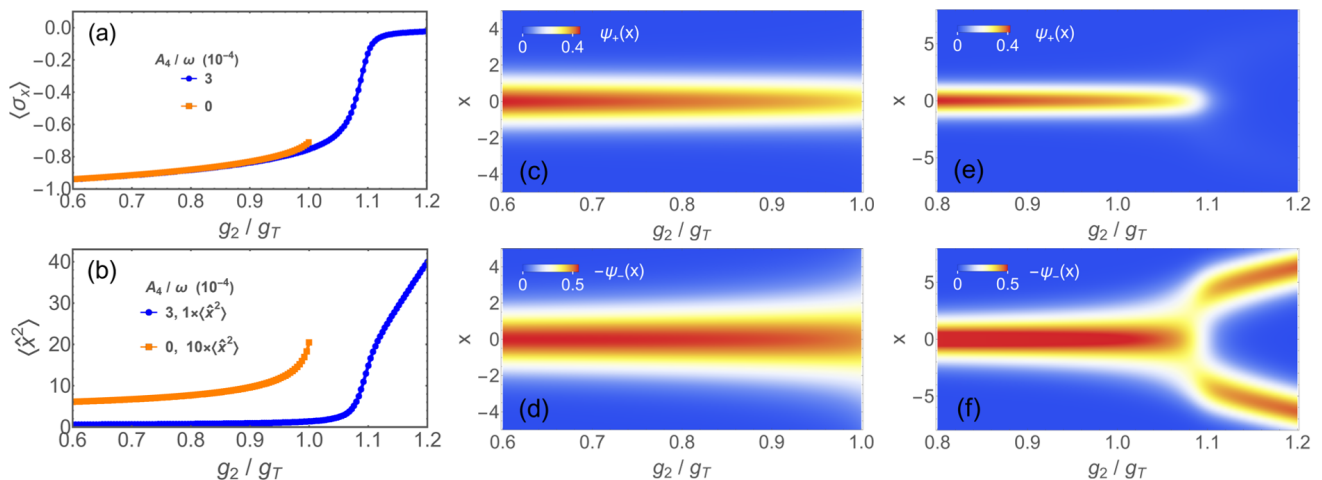


FIG. 5. Resource of sensitivity for critical quantum metrology. (a,b) $\langle \hat{\sigma}_x \rangle$ (a) and $\langle \hat{x}^2 \rangle$ (b) at $A_4 = 0$ [orange (light gray) squares] and $A_4 = 0.0003$ [blue (dark gray) dots]. In (b) the plot of $\langle \hat{x}^2 \rangle$ is amplified by 10 times for $A_4 = 0$. (c-f) Evolution of the wave-function components $\psi_+(x)$ (c,e) and $\psi_-(x)$ (d,f) with respect to g_2 at $A_4 = 0$ (c,d) and $A_4 = 0.0003$ (e,f). Here, $\omega = 1.0\Omega$ in all panels.

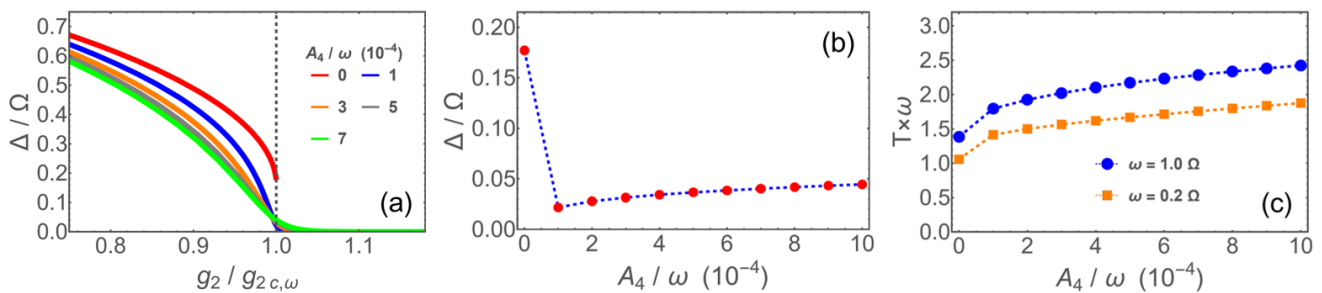


FIG. 6. Finite gap and preparation time for probe state (PTPS). (a) Evolution of the gap Δ with respect to the coupling g_2 at different values of A_4 . (b) Δ at $g_{2c,\omega}$ versus A_4 . Here, $\omega = 1.0\Omega$ in (a) and (b). (c) Dependence of the PTPS (T) on A_4 at different frequencies.

A.

V. QUANTUM FISHER INFORMATION FOR NON-LINEAR CRITICAL QUANTUM METROLOGY

In Fig. 3(c) we have compared the analytic expression (10) for g_{2c} with the peak position of the QFI which takes the following form for a pure state $\psi(\lambda)$ [144–146]

$$F_Q = 4 \left[\langle \psi'(\lambda) | \psi'(\lambda) \rangle - |\langle \psi'(\lambda) | \psi(\lambda) \rangle|^2 \right] \quad (14)$$

where $'$ denotes the derivative with respect to the system parameter λ . In quantum metrology the measurement precision of experimental estimation of the parameter λ is bounded from below by $F_Q^{-1/2}$ [144], with a higher QFI meaning a higher measurement precision. The QFI also corresponds to the susceptibility of the fidelity F via relation $\chi_F = F_Q/4$ [147–149],

$$F = |\langle \psi(\lambda) | \psi(\lambda + \delta\lambda) \rangle| = 1 - \frac{\delta\lambda^2}{2} \chi_F, \quad (15)$$

for an infinitesimal parameter variation $\delta\lambda$. Thus the appearance of a peak in the QFI not only indicates the optimal condition for the metrological application of the system [27, 89, 150, 151] but also the transition point itself [147–149, 152, 153], as demonstrated in [44]. We note here that the second term in (14) vanishes and the expression for F_Q simplifies as

$$F_Q = 4 \langle \psi'(\lambda) | \psi'(\lambda) \rangle \quad (16)$$

for a real wave function $|\psi(\lambda)\rangle$, which describes non-degenerate states of real Hamiltonians [44].

Figure 4(a) shows the QFI around the transition for different values of A_4 and finite frequency $\omega = \Omega$. The parameter λ to be measured is $\lambda = g_2$. In the figure, the coupling strength g_2 is rescaled by the peak position $g_{2c,\omega}$. The QFI becomes exponentially large around $g_{2c,\omega}$ (the y -axis in Fig. 4(a) has a logarithmic scale), meaning very high precision. The Cramér-Rao lower bound for the error [144], $E_{CR} = F_Q^{-1/2}$, is small around $g_{2c,\omega}$ as shown in Fig. 4(b). Remarkably, adding a small A_4 -term leads to a higher peak value of the measurement preci-

sion than the case without regulator, $A_4 = 0$. Furthermore, for $A_4 \neq 0$ (but sufficiently small), F_Q diverges for $\omega \rightarrow 0$, while F_Q for $A_4 = 0$ decreases, as seen in Fig. 4(c). This shows that adding a small quartic term can dramatically improve the measurement precision in quantum metrology.

VI. MECHANISM FOR THE ENHANCED PRECISION

We may clarify the mechanism behind the much higher precision reached by adding a small A_4 term resorting to the variation of the ground state wave function with the parameter $\lambda = g_2$. We compare the expectation values of $\langle \sigma_x \rangle$ and $\langle \hat{x}^2 \rangle$ in Figs. 5(a) and 5(b) at finite frequency $\omega = 1.0\Omega$ as functions of g_2 . For $A_4 = 0$, both $\langle \sigma_x \rangle$ and $\langle \hat{x}^2 \rangle$ show a cusp in the vicinity of the spectral collapse point $g_2 = g_T$, clearly visible in the amplified plot of $\langle \hat{x}^2 \rangle$ in Fig. 5(b). For $g_2 > g_T$, the system becomes unstable and has no longer a ground state. In contrast, for $A_4 \neq 0$, $\langle \sigma_x \rangle$ and $\langle \hat{x}^2 \rangle$ show critical behavior with a sign change of the their second derivative at a coupling value g_{2c} slightly larger than g_T , but no instability.

The sensitivity difference is rooted in the distinct pattern of variation of the wave function with g_2 , as it enters directly the formula for the QFI in (14). Figs. 5(c)-5(f) show the evolution of the two components $\psi_{\pm}(x)$ of the ground state wave function with respect to the coupling g_2 in the absence [Figs. 5(c) and 5(d)] and presence [Figs. 5(e) and 5(f)] of the A_4 -term. We see that for $A_4 = 0$, the wave function ψ_+ (ψ_-) is slightly narrowing (broadening), while approaching the spectral collapse point $g_2 = g_T$. Such wave packet narrowing and broadening are driven by the potential narrowing and broadening due to the frequency renormalization factor $(1 \pm g_2/g_T)$ in Equ. (5), as also plotted in Fig. 2(a) and are also a consequence of the fact that ψ_+ and ψ_- are mutual Fourier transforms of each other for $g_2 = g_T$ [114]. In contrast, the wave-function variation in the presence of the A_4 term is coming not only from the frequency renormalization but also from the wave-packet bifurcating and rapid shifting away from the origin, as in Fig. 2(f). The wave-packet shifting leads to a faster change with g_2 than the mere narrowing and broadening, thus entailing a larger value of $\langle \psi'(\lambda) | \psi'(\lambda) \rangle$ and therefore a higher sensitivity. As a result, a much higher measurement precision is reached for $A_4 \neq 0$.

VII. FINITE GAP AND PREPARATION TIME FOR THE PROBE STATE

Besides the measurement precision characterized by the QFI another aspect important for the practical implementation of quantum metrology is the preparation time for the probe state (PTPS) [27, 72, 89, 93]. The PTPS in critical quantum metrology is determined by

the gap between ground state and first excited state, with longer PTPS needed for smaller gaps. In the linear QRM the PTPS diverges at the critical point due to the exponentially fast closing of the gap in the slow-mode limit [27, 89, 93]. This problem can be remedied by using a mixed model with both linear and quadratic light-matter interactions present [89], leading to a finite PTPS at the critical point.

Here we find that the PTPS is finite both in the absence and presence of the A_4 term. We present the gap evolution with respect to the coupling g_2 for different strengths of A_4 in Figs. 6(a,b). We see that the gap is finite in all cases at $g_{2c,\omega}$ where the QFI reaches the maximum. The PTPS can be estimated as [27, 89]

$$T = \int_0^1 \frac{1}{\Delta(\bar{g}_2)} d\bar{g}_2 \quad (17)$$

where $\bar{g}_2 = g_2/g_{2c,\omega}$. Despite the larger gap for $A_4 = 0$, the PTPS stays always finite and has the same order for zero and finite A_4 , as seen in Fig. 6(c). Note here that, although the PTPS is inversely proportional to the frequency, the PTPS is still finite in our case because the collapse instability from the quadratic term provides a critically enhanced sensitivity resource without requiring the limit $\omega \rightarrow 0$ [89]. Remarkably, this feature persists upon adding the A_4 -term which removes the instability and even leads to a larger QFI as compared to the conventional two-photon QRM. One may thus realize much higher orders of measurement precision without paying the price of a diverging PTPS.

VIII. CONCLUSIONS

In this work we have studied a quadratically coupled QRM with an additional regulator term, quartic in the boson operators, with focus on its application to non-linear critical quantum metrology. The ‘‘spectral collapse’’ phenomenon of the standard two-photon QRM does no longer occur and the spectrum stays bounded from below and purely discrete for all parameter values. The introduction of the quartic A_4 term induces a quantum phase transition in the low-frequency limit, for which we have obtained the phase boundary line analytically. The formula shows a fractional power law in the dependence of the coupling strength. The phase transition extended for finite frequency ratio can be employed for non-linear critically enhanced quantum metrology. Indeed, by examining the QFI we find that adding the A_4 term can yield a much higher order of measurement precision than the conventional two-photon QRM. This enhanced precision is shown to be caused by the different pattern of variation of the ground state wave function while tuning through the transition. Finally we have checked the excitation gap and the PTPS. It turns out that the PTPS is finite both in the absence or presence of the A_4 term. Therefore, adding the A_4 term leads

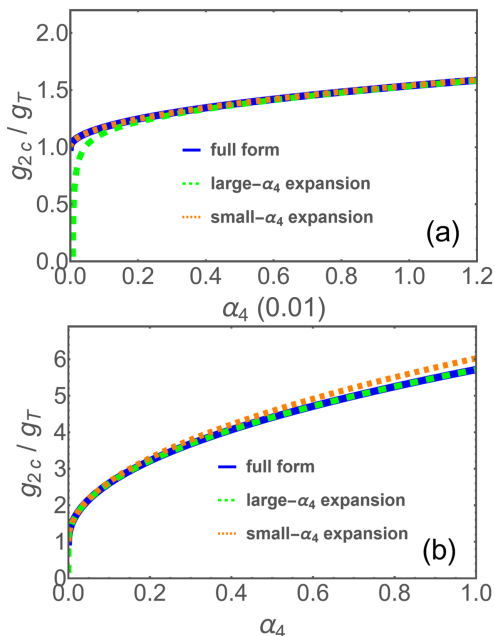


FIG. 7. Comparison of g_{2c} expressions in the full form [Eq. (10), blue solid line] and the expansion forms by small- α_4 expansion [Eq. (12), orange dotted line] and large- α_4 expansion [Eq. (13), green dashed line]. (a) $\alpha_4 \in [0, 0.012]$ (b) $\alpha_4 \in [0, 1]$.

to a metrology protocol which exhibits a strongly enhanced measurement precision compared to the conventional two-photon QRM, while keeping the same *finite*

value of the PTPS. As a final remark we would like to mention that the proposed quadratic QRM with the additional quartic term can be realized in superconducting circuit systems using current technology.

ACKNOWLEDGMENTS

This work was supported by the National Natural Science Foundation of China (Grants No. 12474358, No. 11974151, and No. 12247101). S.F. acknowledges financial support from PNR MUR project PE0000023-NQSTI financed by the European Union - Next Generation EU. D.B. acknowledges support from the German Research Foundation (DFG) under grant No. 439943572.

Appendix A: Comparison of g_{2c} expressions in full form and expansion forms

In Fig. 7, we compare the g_{2c} expressions in the full form [Eq. (10), blue solid line] and the expansion forms by small- α_4 expansion [Eq. (12), orange dotted line] and large- α_4 expansion [Eq. (13), green dashed line]. Indeed, for the $\alpha_4 \in [0, 0.01]$ regime in Fig. 7(a) we see that expansion (12) reproduces the full-form result, while expansion (13) has some qualitative deviations in the small- α_4 limit. For the $\alpha_4 \in [0.01, \infty]$ regime illustrated in Fig. 7(b), expansion (13) works very well for the entire regime, while expansion (12) has some considerable deviations.

-
- [1] M. G. A. Paris, *Int. J. Quantum Inf.* **07**, 125 (2009).
 - [2] C. L. Degen, F. Reinhard, and P. Cappellaro, *Rev. Mod. Phys.* **89**, 035002 (2017).
 - [3] P. Zanardi, M. G. A. Paris, and L. Campos Venuti, *Phys. Rev. A* **78**, 042105 (2008).
 - [4] P. A. Ivanov and D. Porras, *Phys. Rev. A* **88**, 023803 (2013).
 - [5] M. Bina, I. Amelio, and M. G. A. Paris, *Phys. Rev. E* **93**, 052118 (2016).
 - [6] S. Fernández-Lorenzo and D. Porras, *Phys. Rev. A* **96**, 013817 (2017).
 - [7] P. A. Ivanov, *Phys. Rev. A* **102**, 052611 (2020).
 - [8] C. Invernizzi, M. Korbman, L. Campos Venuti, and M. G. A. Paris, *Phys. Rev. A* **78**, 042106 (2008).
 - [9] S. S. Mir Khalaf, E. Witkowska, and L. Lepori, *Phys. Rev. A* **101**, 043609 (2020).
 - [10] A. Niezgoda and J. Chwedeńczuk, *Phys. Rev. Lett.* **126**, 210506 (2021).
 - [11] G. Di Fresco, B. Spagnolo, D. Valenti, and A. Carollo, *SciPost Phys.* **13**, 077 (2022).
 - [12] G. Di Fresco, B. Spagnolo, D. Valenti, and A. Carollo, *Quantum* **8**, 1326 (2024).
 - [13] A. Sahoo, U. Mishra, and D. Rakshit, *Phys. Rev. A* **109**, L030601 (2024).
 - [14] M. Tsang, *Phys. Rev. A* **88**, 021801(R) (2013).
 - [15] K. Macieszczak, M. Guță, I. Lesanovsky, and J. P. Garrahan, *Phys. Rev. A* **93**, 022103 (2016).
 - [16] A. Cabot, F. Carollo, and I. Lesanovsky, *Phys. Rev. Lett.* **132**, 050801 (2024).
 - [17] G. Zicari, M. Carlesso, A. Trombettoni, and M. Patermostro, arXiv preprint arXiv:2407.09304 (2024).
 - [18] M. M. Rams, P. Sierant, O. Dutta, P. Horodecki, and J. Zakrzewski, *Phys. Rev. X* **8**, 021022 (2018).
 - [19] V. Montenegro, U. Mishra, and A. Bayat, *Phys. Rev. Lett.* **126**, 200501 (2021).
 - [20] R. Salvia, M. Mehboudi, and M. Perarnau-Llobet, *Phys. Rev. Lett.* **130**, 240803 (2023).
 - [21] C. Mukhopadhyay and A. Bayat, *Phys. Rev. Lett.* **133**, 120601 (2024).
 - [22] D.-S. Ding, Z.-K. Liu, B.-S. Shi, G.-C. Guo, K. Mølmer, and C. S. Adams, *Nat. Phys.* **18**, 1447 (2022).
 - [23] R. Liu, Y. Chen, M. Jiang, X. Yang, Z. Wu, Y. Li, H. Yuan, X. Peng, and J. Du, *npj Quantum Inf.* **7**, 170 (2021).
 - [24] K. Petrovnin, J. Wang, M. Perelshtein, P. Hakonen, and G. S. Paraoanu, *PRX Quantum* **5**, 020342 (2024).
 - [25] G. Beaulieu, F. Minganti, S. Frasca, M. Scigliuzzo, S. Felicetti, R. Di Candia, and P. Scarlino, arXiv

- preprint arXiv:2409.19968 (2024).
- [26] Y. Yu, R. Liu, G. Xue, C. Yang, C. Wang, J. Zhang, J. Cui, X. Yang, J. Li, J. Han, and H. Yu, (2025), arXiv:2501.04955 [quant-ph].
- [27] L. Garbe, M. Bina, A. Keller, M. G. A. Paris, and S. Felicetti, *Phys. Rev. Lett.* **124**, 120504 (2020).
- [28] S. Ashhab, *Phys. Rev. A* **87**, 013826 (2013).
- [29] Z.-J. Ying, M. Liu, H.-G. Luo, H.-Q. Lin, and J. Q. You, *Phys. Rev. A* **92**, 053823 (2015).
- [30] M.-J. Hwang, R. Puebla, and M. B. Plenio, *Phys. Rev. Lett.* **115**, 180404 (2015).
- [31] M.-J. Hwang and M. B. Plenio, *Phys. Rev. Lett.* **117**, 123602 (2016).
- [32] E. K. Irish and J. Larson, *J. Phys. A: Math. Theor.* **50**, 174002 (2017).
- [33] M. Liu, S. Chesi, Z.-J. Ying, X. Chen, H.-G. Luo, and H.-Q. Lin, *Phys. Rev. Lett.* **119**, 220601 (2017).
- [34] Z.-J. Ying, L. Cong, and X.-M. Sun, *Journal of Physics A: Mathematical and Theoretical* **53**, 345301 (2020), arXiv:1804.08128.
- [35] Z.-J. Ying, *Phys. Rev. A* **103**, 063701 (2021).
- [36] J. Liu, M. Liu, Z.-J. Ying, and H.-G. Luo, *Adv. Quantum Technol.* **4**, 2000139 (2021).
- [37] Z.-J. Ying, *Adv. Quantum Technol.* **5**, 2100088 (2022), [Back Cover (Adv. Quantum Technol. 1/2022): Z.-J. Ying, Adv. Quantum Technol. **5**, 2270013 (2022)].
- [38] Z.-J. Ying, *Adv. Quantum Technol.* **5**, 2100165 (2022).
- [39] Z.-J. Ying, *Adv. Quantum Technol.* **6**, 2200068 (2023), [Front Cover (Adv. Quantum Technol. 1/2023): Z.-J. Ying, Adv. Quantum Technol. **6**, 2370011 (2023)].
- [40] Z.-J. Ying, *Adv. Quantum Technol.* **6**, 2200177 (2023), [Front Cover: (Adv. Quantum Technol. 7/2023), Z.-J. Ying, Adv. Quantum Technol. **6**, 2370071 (2023)].
- [41] Z.-J. Ying, *Phys. Rev. A* **109**, 053705 (2024).
- [42] Z.-J. Ying, *Adv. Quantum Technol.* **7**, 2400053 (2024), [Front Cover: (Adv. Quantum Technol. 7/2024), Z.-J. Ying, Adv. Quantum Technol. **7**, 2470017 (2024)].
- [43] Z.-J. Ying, *Adv. Quantum Technol.* **7**, 2400288 (2024), [Back Cover: (Adv. Quantum Technol. 10/2024), Z.-J. Ying, Adv. Quantum Technol. **7**, 2470029 (2024)].
- [44] Z.-J. Ying, W.-L. Wang, and B.-J. Li, *Phys. Rev. A* **110**, 033715 (2024).
- [45] R. Grimaudo, A. S. M. a. de Castro, A. Messina, E. Solano, and D. Valenti, *Phys. Rev. Lett.* **130**, 043602 (2023).
- [46] R. Grimaudo, D. Valenti, A. Sergi, and A. Messina, *Entropy* **25**, 187 (2023).
- [47] R. Grimaudo, G. Falci, A. Messina, E. Paladino, A. Sergi, E. Solano, and D. Valenti, *Phys. Rev. Res.* **6**, 043298 (2024).
- [48] G.-L. Zhu, C.-S. Hu, H. Wang, W. Qin, X.-Y. Lü, and F. Nori, *Phys. Rev. Lett.* **132**, 193602 (2024).
- [49] C. Liu and J.-F. Huang, *Sci. China Phys. Mech. Astron.* **67**, 210311 (2024).
- [50] M.-J. Hwang, R. Puebla, and M. B. Plenio, *Phys. Rev. Lett.* **115**, 180404 (2015).
- [51] S. Felicetti and A. Le Boité, *Phys. Rev. Lett.* **124**, 040404 (2020).
- [52] R. Puebla, M.-J. Hwang, J. Casanova, and M. B. Plenio, *Phys. Rev. Lett.* **118**, 073001 (2017).
- [53] J. Peng, E. Rico, J. Zhong, E. Solano, and I. L. Egusquiza, *Phys. Rev. A* **100**, 063820 (2019).
- [54] H.-J. Zhu, K. Xu, G.-F. Zhang, and W.-M. Liu, *Phys. Rev. Lett.* **125**, 050402 (2020).
- [55] H.-L. Zhang, J.-H. Lü, K. Chen, X.-J. Yu, F. Wu, Z.-B. Yang, and S.-B. Zheng, *Opt. Express* **32**, 22566 (2024).
- [56] N. Bartolo, F. Minganti, W. Casteels, and C. Ciuti, *Phys. Rev. A* **94**, 033841 (2016).
- [57] F. Minganti, L. Garbe, A. Le Boité, and S. Felicetti, *Phys. Rev. A* **107**, 013715 (2023).
- [58] F. Minganti, V. Savona, and A. Biella, *Quantum* **7**, 1170 (2023).
- [59] G. Liu, W. Xiong, and Z.-J. Ying, *Phys. Rev. A* **108**, 033704 (2023).
- [60] M.-L. Cai, Z.-D. Liu, W.-D. Zhao, Y.-K. Wu, Q.-X. Mei, Y. Jiang, L. He, X. Zhang, Z.-C. Zhou, and L.-M. Duan, *Nat. Commun.* **12**, 1126 (2021).
- [61] A. Delteil, T. Fink, A. Schade, S. Höfling, C. Schneider, and A. Imamoglu, *Nat. Mat.* **18**, 219 (2019).
- [62] Z. Li, F. Claude, T. Boulier, E. Giacobino, Q. Glorieux, A. Bramati, and C. Ciuti, *Phys. Rev. Lett.* **128**, 093601 (2022).
- [63] J. M. Fink, A. Dombi, A. Vukics, A. Wallraff, and P. Domokos, *Phys. Rev. X* **7**, 011012 (2017).
- [64] P. Brookes, G. Tancredi, A. D. Patterson, J. Rahamim, M. Esposito, T. K. Mavrogordatos, P. J. Leek, E. Ginossar, and M. H. Szymanska, *Sci. Adv.* **7**, eabe9492 (2021).
- [65] G. Beaulieu, F. Minganti, S. Frasca, V. Savona, S. Felicetti, R. Di Candia, and P. Scarlino, arXiv preprint arXiv:2310.13636 (2023).
- [66] Q.-M. Chen, M. Fischer, Y. Nojiri, M. Renger, E. Xie, M. Partanen, S. Pogorzalek, K. G. Fedorov, A. Marx, F. Deppe, *et al.*, *Nat. Commun.* **14**, 2896 (2023).
- [67] R. Sett, F. Hassani, D. Phan, S. Barzanjeh, A. Vukics, and J. M. Fink, *PRX Quantum* **5**, 010327 (2024).
- [68] V. Jouanny, S. Frasca, V. J. Weibel, L. Peyruchat, M. Scigliuzzo, F. Oppliger, F. De Palma, D. Sbroglio, G. Beaulieu, O. Zilberberg, *et al.*, arXiv preprint arXiv:2403.18150 (2024).
- [69] Y. Chu, S. Zhang, B. Yu, and J. Cai, *Phys. Rev. Lett.* **126**, 010502 (2021).
- [70] L. Garbe, O. Abah, S. Felicetti, and P. Puebla, *Quantum Sci. Technol.* **7**, 035010 (2022).
- [71] K. Gietka, L. Ruks, and T. Busch, *Quantum* **6**, 700 (2022).
- [72] K. Gietka, *Phys. Rev. A* **105**, 042620 (2022).
- [73] L. Garbe, O. Abah, S. Felicetti, and R. Puebla, *Phys. Rev. Res.* **4**, 043061 (2022).
- [74] T. Ilias, D. Yang, S. F. Huelga, and M. B. Plenio, *PRX Quantum* **3**, 010354 (2022).
- [75] D. Yang, S. F. Huelga, and M. B. Plenio, *Phys. Rev. X* **13**, 031012 (2023).
- [76] U. Alushi, W. Górecki, S. Felicetti, and R. Di Candia, *Phys. Rev. Lett.* **133**, 040801 (2024).
- [77] T. L. Heugel, M. Biondi, O. Zilberberg, and R. Chitra, *Phys. Rev. Lett.* **123**, 173601 (2019).
- [78] R. Di Candia, F. Minganti, K. V. Petrovnin, G. S. Paraoanu, and S. Felicetti, *npj Quantum Inf.* **9**, 23 (2023).
- [79] E. Rinaldi, R. Di Candia, S. Felicetti, and F. Minganti, arXiv preprint arXiv:2112.05332 (2021).
- [80] C. Hotter, H. Ritsch, and K. Gietka, *Phys. Rev. Lett.* **132**, 060801 (2024).
- [81] S. Choi, Y. Salamin, C. Roques-Carmes, J. Sloan, M. Horodyski, and M. Soljacic, arXiv preprint arXiv:2412.01772 (2024).

- [82] U. Alushi, A. Coppo, V. Brosco, R. Di Candia, and S. Felicetti, *Communications Physics* **8**, 74 (2025).
- [83] T. Ilias, D. Yang, S. F. Huelga, and M. B. Plenio, *npj Quantum Inf.* **10**, 36 (2024).
- [84] S.-W. Bin, X.-Y. Lü, T.-S. Yin, G.-L. Zhu, Q. Bin, and Y. Wu, *Opt. Lett.* **44**, 630 (2019).
- [85] S.-B. Tang, H. Qin, B.-B. Liu, D.-Y. Wang, K. Cui, S.-L. Su, L.-L. Yan, and G. Chen, *Phys. Rev. A* **108**, 053514 (2023).
- [86] Q.-K. Wan, H.-L. Shi, and X.-W. Guan, *Phys. Rev. B* **109**, L041301 (2024).
- [87] G. Mihailescu, A. Bayat, S. Campbell, and A. K. Mitchell, *Quantum Sci. Technol.* **9**, 035033 (2024).
- [88] G. Mihailescu, A. Kiely, and A. K. Mitchell, *arXiv preprint arXiv:2406.18662* (2024).
- [89] Z.-J. Ying, S. Felicetti, G. Liu, and D. Braak, *Entropy* **24**, 1015 (2022).
- [90] D. Xie, C. Xu, and A. M. Wang, *Eur. Phys. J. Plus* **137**, 1323 (2022).
- [91] K. Gietka, C. Hotter, and H. Ritsch, *Phys. Rev. Lett.* **131**, 223604 (2023).
- [92] X. Zhu, J.-H. Lü, W. Ning, L.-T. Shen, F. Wu, and Z.-B. Yang, *Phys. Rev. A* **109**, 052621 (2024).
- [93] Z.-J. Ying, *Adv. Quantum Technol.* **8**, 2400630 (2025).
- [94] Z.-J. Ying, *arXiv:2502.04466* (2025).
- [95] S. Felicetti, J. S. Pedernales, I. L. Egusquiza, G. Romero, L. Lamata, D. Braak, and E. Solano, *Phys. Rev. A* **92**, 033817 (2015).
- [96] S. Felicetti, D. Z. Rossatto, E. Rico, E. Solano, and P. Forn-Díaz, *Phys. Rev. A* **97**, 013851 (2018).
- [97] S. Felicetti, M.-J. Hwang, and A. Le Boité, *Phys. Rev. A* **98**, 053859 (2018).
- [98] R. Gautier, A. Sarlette, and M. Mirrahimi, *PRX Quantum* **3**, 020339 (2022).
- [99] M. Ayyash, X. Xu, S. Ashhab, and M. Mariantoni, *Phys. Rev. A* **110**, 053711 (2024).
- [100] X. Wang, A. Miranowicz, H.-R. Li, and F. Nori, *Physical Review A* **93**, 063861 (2016), publisher: American Physical Society.
- [101] C. Sánchez Muñoz, A. Lara, J. Puebla, and F. Nori, *Physical Review Letters* **121**, 123604 (2018), publisher: American Physical Society.
- [102] L. Cong, S. Felicetti, J. Casanova, L. Lamata, E. Solano, and I. Arrazola, *Physical Review A* **101**, 032350 (2020).
- [103] K. K. W. Ma, *Phys. Rev. A* **102**, 053709 (2020).
- [104] F. Zou, X.-Y. Zhang, X.-W. Xu, J.-F. Huang, and J.-Q. Liao, *Physical Review A* **102**, 053710 (2020).
- [105] N. Piccione, S. Felicetti, and B. Bellomo, *Phys. Rev. A* **105**, L011702 (2022).
- [106] J. Li, R. Fazio, and S. Chesi, *New Journal of Physics* **24**, 083039 (2022).
- [107] J. Li and S. Chesi, *Physical Review A* **109**, 053702 (2024).
- [108] A. J. Shah, P. Kirton, S. Felicetti, and H. Alaeian, “Dissipative phase transition in the two-photon dicke model,” (2024), *arXiv:2412.14271 [quant-ph]*.
- [109] S. Cui, J.-P. Cao, H. Fan, and L. Amico, *Journal of Physics A: Mathematical and Theoretical* **50**, 204001 (2017).
- [110] I. Travěněc, *Phys. Rev. A* **85**, 043805 (2012).
- [111] L. Duan, Y.-F. Xie, D. Braak, and Q.-H. Chen, *Journal of Physics A: Mathematical and Theoretical* **49**, 464002 (2016).
- [112] L. Cong, X.-M. Sun, M. Liu, Z.-J. Ying, and H.-G. Luo, *Phys. Rev. A* **99**, 013815 (2019).
- [113] R. J. A. Rico, F. H. Maldonado-Villamizar, and B. M. Rodríguez-Lara, *Phys. Rev. A* **101**, 063825 (2020).
- [114] D. Braak, *Ann. Phys. (Berlin)* **535**, 2200519 (2023).
- [115] H.-P. Eckle and H. Johannesson, *Journal of Physics A: Mathematical and Theoretical* **50**, 294004 (2017).
- [116] H.-H. Han, Z.-J. Ying, S. Felicetti, and D. Braak, *arXiv* (2025).
- [117] E. K. Irish and J. Gea-Banacloche, *Phys. Rev. B* **89**, 085421 (2014).
- [118] J. E. Mooij, T. P. Orlando, L. Levitov, L. Tian, C. H. van der Wal, and S. Lloyd, *Science* **285**, 1036 (1999).
- [119] C. Ciuti, G. Bastard, and I. Carusotto, *Phys. Rev. B* **72**, 115303 (2005).
- [120] A. A. Anappara, S. De Liberato, A. Tredicucci, C. Ciuti, G. Biasiol, L. Sorba, and F. Beltram, *Phys. Rev. B* **79**, 201303(R) (2009).
- [121] P. Forn-Díaz, L. Lamata, E. Rico, J. Kono, and E. Solano, *Rev. Mod. Phys.* **91**, 025005 (2019).
- [122] A. F. Kockum, A. Miranowicz, S. De Liberato, S. Savasta, and F. Nori, *Nature Reviews Physics* **1**, 19 (2019).
- [123] A. Wallraff, D. I. Schuster, A. Blais, L. Frunzio, R.-S. Huang, J. Majer, S. Kumar, S. M. Girvin, and R. J. Schoelkopf, *Nature* **431**, 162.
- [124] G. Günter, A. A. Anappara, J. Hees, A. Sell, G. Biasiol, L. Sorba, S. De Liberato, C. Ciuti, A. Tredicucci, A. Leitenstorfer, and R. Huber, *Nature* **458**, 178 (2009).
- [125] T. Niemczyk, F. Deppe, H. Huebl, E. P. Menzel, F. Hocke, M. J. Schwarz, J. J. García-Ripoll, D. Zueco, T. Hummer, E. Solano, A. Marx, and R. Gross, *Nat. Phys.* **6**, 772 (2010).
- [126] B. Peropadre, P. Forn-Díaz, E. Solano, and J. J. García-Ripoll, *Phys. Rev. Lett.* **105**, 023601 (2010).
- [127] P. Forn-Díaz, J. J. García-Ripoll, B. Peropadre, J. L. Orgiazzi, M. A. Yurtalan, R. Belyansky, C. M. Wilson, and A. Lupascu, *Nature Physics* **13**, 39 (2017).
- [128] P. Forn-Díaz, J. Lisenfeld, D. Marcos, J. J. García-Ripoll, E. Solano, C. J. P. M. Harmans, and J. E. Mooij, *Phys. Rev. Lett.* **105**, 237001 (2010).
- [129] G. Scalari, C. Maissen, D. Turčínková, D. Hagenmüller, S. De Liberato, C. Ciuti, C. Reichl, D. Schuh, W. Wegscheider, M. Beck, and J. Faist, *Science* **335**, 1323 (2012).
- [130] Z.-L. Xiang, S. Ashhab, J. Q. You, and F. Nori, *Rev. Mod. Phys.* **85**, 623 (2013).
- [131] F. Yoshihara, T. Fuse, S. Ashhab, K. Kakuyanagi, S. Saito, and K. Semba, *Nature Physics* **13**, 44 (2017).
- [132] X. Gu, A. F. Kockum, A. Miranowicz, Y.-X. Liu, and F. Nori, *Physics Reports* **718-719**, 1 (2017).
- [133] J.-F. Huang, J.-Q. Liao, and L.-M. Kuang, *Phys. Rev. A* **101**, 043835 (2020).
- [134] A. Stokes and A. Nazir, *Nat. Commun.* **10**, 499 (2019).
- [135] Q.-T. Xie, S. Cui, J.-P. Cao, L. Amico, and H. Fan, *Phys. Rev. X* **4**, 021046 (2014).
- [136] W. Qin, A. F. Kockum, C. S. Muñoz, A. Miranowicz, and F. Nori, *Physics Reports* **1078**, 1 (2024).
- [137] A. Bayer, M. Pozimski, S. Schambeck, D. Schuh, R. Huber, D. Bougeard, and C. Lange, *Nano letters* **17**, 6340 (2017).
- [138] J. Casanova, G. Romero, I. Lizuain, J. J. García-Ripoll, and E. Solano, *Phys. Rev. Lett.* **105**, 263603 (2010).

- [139] C. F. Lo, K. L. Liu, and K. M. Ng, Europhysics Letters (EPL) **42**, 1 (1998).
- [140] L. Duan, Y.-F. Xie, D. Braak, and Q.-H. Chen, Journal of Physics A: Mathematical and Theoretical **49**, 464002 (2016).
- [141] L. Garbe, I. L. Egusquiza, E. Solano, C. Ciuti, T. Coudreau, P. Milman, and S. Felicetti, Phys. Rev. A **95**, 053854 (2017).
- [142] J. Li, D. Braak, and Q.-H. Chen, arXiv:2412.20437 (2024).
- [143] M. Reed and B. Simon, *II: Fourier analysis, self-adjointness*, Vol. 2 (Elsevier, 1975).
- [144] S. L. Braunstein and C. M. Caves, Phys. Rev. Lett. **72**, 3439 (1994).
- [145] M. M. Taddei, B. M. Escher, L. Davidovich, and R. L. de Matos Filho, Phys. Rev. Lett. **110**, 050402 (2013).
- [146] M. M. Rams, P. Sierant, O. Dutta, P. Horodecki, and J. Zakrzewski, Phys. Rev. X **8**, 021022 (2018).
- [147] S.-J. GU, International Journal of Modern Physics B **24**, 4371 (2010).
- [148] W.-L. You, Y.-W. Li, and S.-J. Gu, Phys. Rev. E **76**, 022101 (2007).
- [149] W.-L. You and L. He, Journal of Physics: Condensed Matter **27**, 205601 (2015).
- [150] L. Garbe, O. Abah, S. Felicetti, and R. Puebla, Phys. Rev. Res. **4**, 043061 (2022).
- [151] T. Ilias, D. Yang, S. F. Huelga, and M. B. Plenio, PRX Quantum **3**, 010354 (2022).
- [152] H.-Q. Zhou and J. P. Barjaktarevič, Journal of Physics A: Mathematical and Theoretical **41**, 412001 (2008).
- [153] P. Zanardi and N. Paunković, Phys. Rev. E **74**, 031123 (2006).